The performance of Marciniak – Kuczinsky approach on prediction of plastic instability of metals subjected to complex loadings

IOP Conf. Series: Journal of Physics: Conf. Series **1063** (2018) 012061 doi:10.1088/1742-6596/1063/1/012061

The performance of Marciniak – Kuczinsky approach on prediction of plastic instability of metals subjected to complex loadings

M.C. Butuc and G. Vincze*

[1]Centre for Mechanical Technology and Automation, University of Aveiro, Campus Universitário de Santiago, 3810-193 Aveiro, Portugal

E-mail: gvincze@ua.pt

Abstract. The objective of the present paper is to analyse the performance of Marciniak-Kuczinsky (MK) theory on the prediction of formability of sheet metals subjected to complex loadings. Advanced constitutive equations taking into account isotropic and anisotropic hardening are applied to describe the material mechanical behaviour under linear and complex loadings. A comparative study on their accuracy on predicting the forming limits for the studied material is performed. Two deep-drawing quality sheet metals are selected. Several strain path changes are taken into account. A good agreement between the theoretical and experimental results was obtained. MK theory is an efficient and valuable tool on the prediction of plastic flow localization of sheet metals under complex loadings when proper constitutive equations are used.

1. Introduction

The forming limit diagram (FLD) introduced by Keeler [1] and Goodwin [2] is a constructive concept for characterizing the formability of sheet metals. It is essential for material selection, design and try out of the tools for deep drawing operations. Sheet metal forming processes involve forming sequences with severe strain-path changes that drastically influence the forming limits. For non proportional strain paths, FLDs are very useful to understand the behaviour of the material upon complex loading, to estimate the severity of the strain paths imposed to the work-piece and to optimise the shape of the dies to avoid necking. The theoretical prediction of FLDs under complex loadings is of great interest since the experimentally determination involves a complex work. Marciniak-Kuczinsky (MK) approach [3] has become one of the most important tools in predicting the sheet metal formability. The predicted limit strains strongly depend on the constitutive law incorporated in the MK analysis [4-7]. In the present work an advanced model for predicting the forming limits of sheet metal under linear and complex strain paths involving sequences of two linear strain paths is used to analyse the performance of MK theory in predicting the plastic instability in complex loadings.

2. Theoretical computation of Forming Limit Diagram

The simulation of plastic instability is carried out by using a Marciniak-Kuczinsky-type analysis. The model is based on the growth by plastic deformation within a thin sheet of an initial defect in the form of a groove-like, narrow band of diminished thickness. Following the Hutchinson-Neal model the initial inclination angle of the band with respect to the minor principal axis of the stress tensor is denoted by ψ_0. It is supposed that the material has a rigid-plastic, rate-independent behaviour. Isotropic and anisotropic hardening models are considered to describe the hardening behaviour of material. The initial shape of the yield locus is generated by the anisotropic Yld2000-2d plane stress yield function. A plane stress condition is assumed throughout. Small increments of equivalent strain are imposed in the homogeneous region, the corresponding stress and strain states being computed according to the algorithm presented by Butuc *et al*. [8]. In order to define the strain and stress states within the band, the Newton-Raphson method is applied for solving a system of two polynomial functions resulting from the yield criterion and the requirement of deformation compatibility in the longitudinal direction of the necking band. When the effective strain increment in the band becomes 10 times greater than the one in the homogeneous zone, the analysis assumes that plastic flow localization occurs, whereas the accumulated principal strains in the homogeneous zone define the forming strain limits. For each considered strain path, the analysis is repeated for different values of ψ_0 (between 0 and 90 degrees) and the limit point on the FLD is obtained through the minimization of the principal strain in the homogeneous zone, versus ψ_0. The simulation of the complex strain paths involves a prestrain of the homogeneous zone followed by a change in strain path. The sheet metal is unloaded to a zero-stress state after the prestrain and subsequently reloaded following the second strain path. The prestrain is accounted for when considering the evolution of the internal variables of the microstructural hardening model and in the equivalent plastic strain for the cases involving the Voce and Swift hardening laws, respectively.

2.1. Isotropic hardening models

The isotropic strain hardening component is expressed by the Swift model in the form of a power law

$$\bar{\sigma} = K\left(\varepsilon_0 + \bar{\varepsilon}\right)^n \tag{1}$$

and by the Voce saturation strain-hardening law :

$$\bar{\sigma} = A - B\exp\left(-C\bar{\varepsilon}\right) \tag{2}$$

2.2. Microstructural hardening model

The microstructural hardening model of Teodosiu and Hu [9] (acronym MicMod) describes the hardening of the material by four internal state variables denoted by $\{R, \boldsymbol{X}, \boldsymbol{S}, \boldsymbol{P}\}$.The evolution laws of the internal state variables are written in a work-hardening/recovery format, reflecting the dynamic processes of the production/annihilation of dislocations and of the formation/dissolution of dislocation structures. The evolution equations are:

$$\sigma = Y_0 + R + mS \tag{3}$$

$$S = |\boldsymbol{S}| = \left|\sqrt{S_{\mathrm{L}}^2 + S_{\mathrm{D}}^2}\right| ;\ \dot{R} = C_R\left(R_{sat} - R\right)\dot{\bar{\varepsilon}} ,\ \dot{\mathbf{P}} = C_{\mathrm{P}}\left(\mathbf{A} - \mathbf{P}\right)\dot{\bar{\varepsilon}}$$

$$\dot{\mathbf{X}} = C_{\mathrm{X}}\left(\frac{\bar{X}_{\mathrm{sat}}}{\bar{\sigma}_{\mathbf{e}}}\left(\boldsymbol{\sigma}'-\mathbf{X}\right) - \mathbf{X}\right)\dot{\bar{\varepsilon}};\ \bar{X}_{\mathrm{sat}} = X_0 + \left(1-m\right)\sqrt{S_{\mathrm{D}}^2 + q\left|\boldsymbol{S}_{\mathrm{L}}\right|^2}$$

$$\boldsymbol{S} = S_{\mathrm{D}}\,\boldsymbol{A}\otimes\boldsymbol{A} + \boldsymbol{S}_{\mathrm{L}} ;\ \dot{S}_D = C_{SD}\left[h_P\left(S_{sat} - S_D\right) - h_X S_D\right]\dot{\bar{\varepsilon}}$$

$$h_{\mathrm{X}} = \frac{1}{2}\left(1 - \frac{\mathbf{X}:\boldsymbol{A}}{\overline{\mathrm{X}}_{\mathrm{sat}}\left(\boldsymbol{\sigma}'-\mathbf{X}\right):\boldsymbol{A}}\overline{\boldsymbol{\sigma}}_{\mathrm{e}}\right);\ h_{\mathrm{P}} = \begin{cases} 1 - \dfrac{C_{\mathrm{P}}}{C_{\mathrm{SD}}+C_{\mathrm{P}}}\left|\dfrac{S_{\mathrm{D}}}{S_{\mathrm{sat}}} - \boldsymbol{P}:\boldsymbol{A}\right| & \text{, if } \boldsymbol{P}:\boldsymbol{A} \geq 0 \\ \left(1+\boldsymbol{P}:\boldsymbol{A}\right)^{\mathrm{n_P}}\left(1 - \dfrac{C_{\mathrm{P}}}{C_{\mathrm{SD}}+C_{\mathrm{P}}}\dfrac{S_{\mathrm{D}}}{S_{\mathrm{sat}}}\right) & \text{, otherwise.} \end{cases} \tag{4}$$

$$\dot{\boldsymbol{S}}_{\mathrm{L}} = -C_{\mathrm{SL}}\left(\frac{\left|\boldsymbol{S}_{\mathrm{L}}\right|}{S_{\mathrm{sat}}}\right)^{\mathrm{n_L}}\boldsymbol{S}_{\mathrm{L}}\,\dot{\bar{\varepsilon}} \tag{5}$$

The model involves 13 material parameters: τ_0, X_0, S_{sat}, R_{sat}, $C_{\mathrm{p}}C_{\mathrm{P}}$, C_{SL}, C_{SD}, C_{X}, C_{R}, $n_{\mathrm{p}}n_{\mathrm{P}}$, n_{L}, m and q. The simplified version of microstructural hardening model of Teodosiu et Hu [10] appropriated for aluminium alloys considers that the directionality effects of the dislocation structures for aluminium alloys are almost absent and their contribution to the isotropic hardening is described by a scalar internal variable (S). The simplified evolution equations are:

$$\overline{X}_{sat} = X_0 + \left(1-m\right)S \tag{6}$$

$$\dot{S} = C_S\left(S_{sat} - S\right)\dot{\bar{\varepsilon}}, \qquad S(0)=0 \tag{7}$$

The simplified microstructural model involves 8 material parameters: Y_0, f, C_{R}, R_{sat}, C_{X}, X_0, C_S, $Ssat$. The detailed description of the microstructural model and the information about the identification of the parameters involved are found in [9] and [10].

2.3 YLD2000-2D Yield Function

The Yld2000-2d [11] plane stress yield function (acronym YLD00-2d) introduces plastic anisotropy with two linear transformations on the Cauchy stress tensor. It is expressed in terms of the deviatoric stress components as:

$$\phi = \phi'\left(\boldsymbol{S}'\right) + \phi''(\boldsymbol{S}'') = 2\overline{\sigma}_{\mathrm{Y}}^{a} \tag{8}$$

where $\overline{\sigma}_{\mathrm{Y}}$ is the effective stress, a is an exponent connected to the crystal structure, ϕ' and ϕ'' are two isotropic functions defined by

$$\phi'(\tilde{\boldsymbol{S}}') = \left|\tilde{S}'_1 - \tilde{S}'_2\right|^{a} \tag{9}$$

$$\phi''(\tilde{\boldsymbol{S}}'') = \left|2\tilde{S}''_2 + \tilde{S}''_1\right|^{a} + \left|2\tilde{S}''_1 + \tilde{S}''_2\right|^{a} \tag{10}$$

$\tilde{\boldsymbol{S}}'$ and $\tilde{\boldsymbol{S}}''$ are the linear transformations of the effective stress tensor $\boldsymbol{s}$ defined as the deviatoric part $\boldsymbol{\sigma}'$ of the Cauchy stress:

$$\tilde{\boldsymbol{S}}' = \boldsymbol{C}'\boldsymbol{s},\ \tilde{\boldsymbol{S}}'' = \boldsymbol{C}''\boldsymbol{s} \tag{11}$$

where $\boldsymbol{C}'$ and $\boldsymbol{C}''$ contain the material anisotropy coefficients.

3. Results and discussion

Two materials of deep-drawing quality have been considered in our study, namely AA6016-T4 aluminium alloy and a bake-hardened steel (BH steel). The coefficients of the selected models are obtained by numerical identifications from the experimental data. Table 1 shows the values of the coefficients of the YLD00-2d yield function. Table 2 contains the material parameters involved in the microstructural hardening model. It is mentioned that the AA6016-T4 parameters of the microstructural model are used from [10].

Table 1. The coefficients of YLD00-2d yield function

Material	a	α_1	α_2	α_3	α_4	α_5	α_6	α_7	α_8
AA6016	8	0.88	1.157	0.933	1.097	1.018	1.003	0.933	1.061
BH steel	6	1.072	1.039	1.027	0.916	0.943	1.0423	0.982	0.837

Table 2. The material parameters of the microstructural model

Parameters	Y_0	C_R	R_{sat}	C_X	X_0	$C_{SD}/^*C_S$	C_{SL}	S_{sat}	n_L	n_p	q	m	C_P
AA6016	124.2	35.6	36.9	244.2	14.5	7.9	-	158.8	-	-	-	0.613	-
BH steel	202.93	37.2	73.45	160.15	2.33	4.93	5.575	229.8	0.25	24.05	1.855	0.297	3.5

By fitting experimental true stress – true plastic strain data measured in uniaxial test along RD, the Voce equation was identified for AA6016-T4 as: $\bar{\sigma}(\bar{\varepsilon}) = 318.103 - 191.103\exp(-8.706\bar{\varepsilon})$ and the Swift equation was identified for BH steel sheet as: $\bar{\sigma}(\bar{\varepsilon}) = 548.67(0.01+\bar{\varepsilon})^{0.195}$

The experimental FLDs of the present analysis, involve the experimental forming limits obtained for linear strain paths (LSP) namely, uniaxial tension (UT), plane strain (PS) and biaxial stretching (BS) with circular and elliptical die rings, and for complex strain paths namely, uniaxial tension at 0º and 90º from RD (at 7% and 14%) followed by biaxial stretching (UT-BS; UT_90º-BS), biaxial stretching (at 5%) followed by uniaxial tension (BS-UT), uniaxial tension at 0º and 90º from RD (at 7% and 14%) followed by stretching with different elliptical die rings (UT-X; UT_90º-X). The acronym X represents different strain paths between UT and BS, expressed theoretically by different stress ratio "α". The theoretical FLDs under non-proportional loading (UT/UT_90-X) involve a sequence of two linear strain paths, keeping constant the preliminary strain ratio and the amount of prestrain and varying the subsequent strain ratio. Specifically, it was considered prestrains at 7% and 14% under uniaxial tension at 0º and 90º from RD (UT/UT_90º) followed by different strain paths (acronym X) between UT and BS.

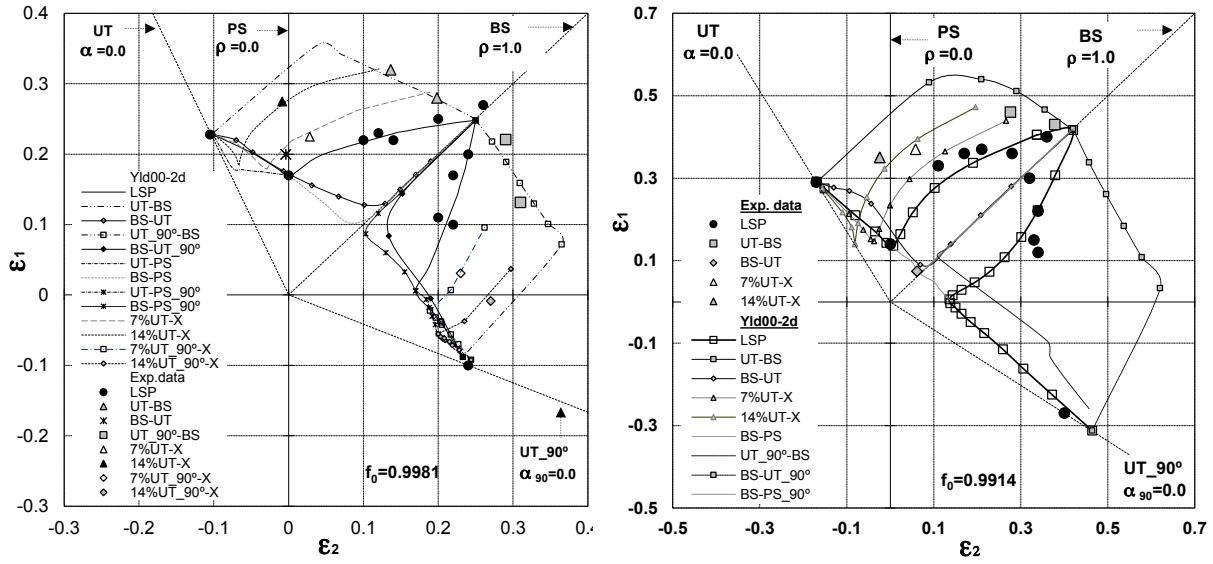

a)YLD00-2d_Voce b)YLD00-2d Swift

Figure 1.: FLDs under linear and complex strain paths for a) AA6016-T4 and b) BH steel

Fig. 1 shows the experimental forming limits for AA6016-T4 aluminium alloy and BH steel under proportional and non-proportional loading and the computed ones, obtained by YLD00-2d yield criterion coupled with Voce law and Swift law, respectively. The predicted curves show a very good agreement with the experimental results in both linear strain path and strain path changes for sheet samples cut along rolling and transverse direction.

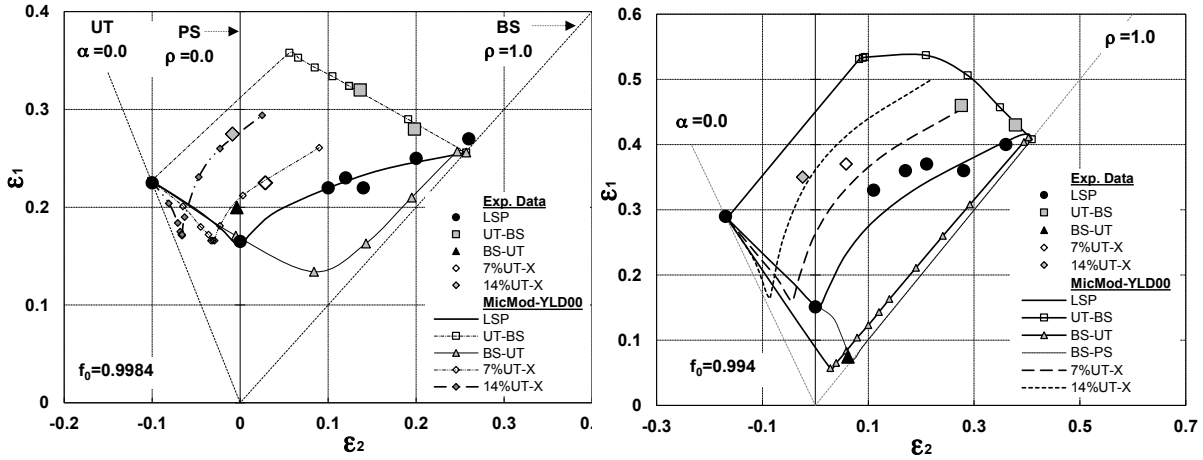

a) AA6016-T4 aluminum alloy **b)** BH steel sheet

Figure 2.: Experimental and theoretical FLDs predicted by MicMod_Yld00

Figure 2a depicts the experimental forming limits for AA6016-T4 sheet for linear and complex strain paths and the theoretical limits predicted by using YLD00-2d yield function and the simplified version of microstructural hardening model. For aluminum alloys the decrease of formability under a biaxial stretching followed by uniaxial tension is not so pronounced like for steel sheet. The simplified version of the microstructural hardening model coupled with YLD00-2d yield function allows very good results, similar with those obtained with Voce saturation hardening law. Figure 2b shows the experimental forming limits for BH steel under proportional and non-proportional loading and the computed ones, when the shape of yield surface is described by the YLD00-2d yield function and the hardening model is expressed by microstructural hardening model. The performance of modeling the material hardening on the basis of the microstructure evolution consists on predicting a more accentuate decrease of forming limits under a strain history involving a biaxial stretching prestrain followed by a uniaxial tension.

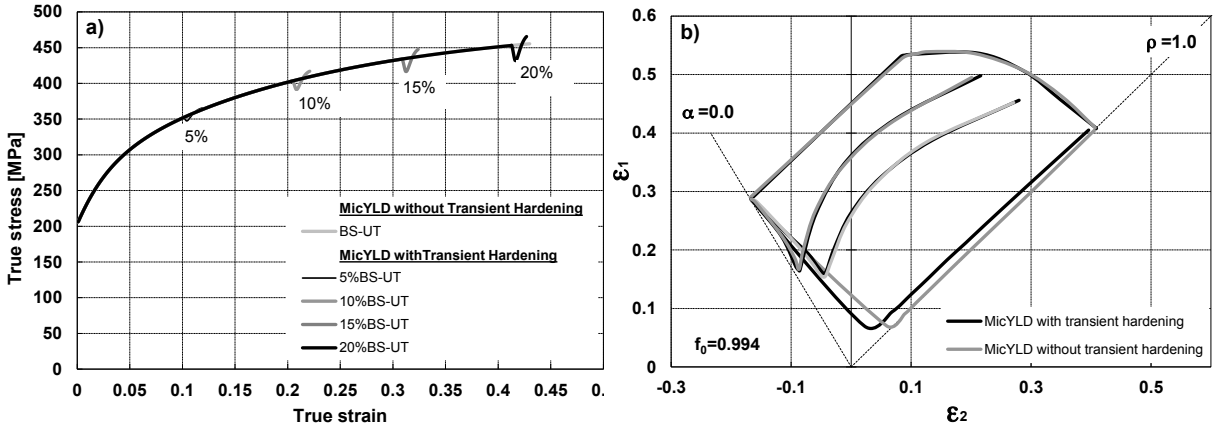

Figure 3.: The effect of the transient hardening in a) the true stress –trues strain curve under BS-UT strain path change and b) the complex FLDs of BH steel sheet

Figure 3a shows the effect of the transient hardening captured by the microstructural model on the true stress–true strain curve under BS-UT loading at different values of prestrains. Figure 3b shows that the transient hardening effect is noticed only in the BS-UT strain path. These results confirm that the additional drop on formability predicted by microstructural model by comparing with Swift hardening law under uniaxial tension reloading after biaxial prestrain can be ascribed to the occurrence of the transient hardening as mentioned by Hiwatashi et al [12] and Hoferlin et al [13], possibly as a consequence of the interaction between the currently active slips and the previously formed dislocation structures as suggested by Rauch and Schmitt [14].

For both selected materials a very good agreement is observed between theoretical and experimental forming limits for linear and complex strain paths. The FLDmodel captured the significant increase of formability in uniaxial prestrain followed by biaxial stretching, the premature instability for biaxial prestrain followed by uniaxial tension as well as the experimental tendencies for UT-X strain path changes. The main advantage of modeling the material hardening of BH steel on the basis of the microstructure evolution consists on reproducibility of Nakazima experimental tendency for steels by predicting the forming limit curve under equibiaxial stretching prestrain followed by uniaxial tension as the lowest curve on the forming limit diagram.

4. Conclusions

An advanced sheet metal forming limit model under linear and complex strain paths, based on Marciniak-Kuczinsky analysis, was presented. The advanced phenomenological anisotropic yield criterion YLD00-2d coupled with Voce saturation strain-hardening law, Swift strain–hardening power law and microstructural hardening model of Teodosiu and Hu, respectively, have been used to predict the forming limits for AA6016-T4 aluminium alloy sheet and for a bake hardened steel sheet, respectively, under linear and several two-stage strain path changes. A very good agreement between experiments and theoretical results predicted by all selected models has been found. The presented study showed that the MK approach is a valuable and practical tool to predict and analyze the sheet metal formability under linear and complex loadings when appropriate constitutive equations are applied.

Acknowledgments

The authors acknowledge support from the Portuguese Foundation of Science and Technology (FCT) through projects UID/EMS/00481/2013 and POCI-01-0145-FEDER-032466. Especial thanks are expressed to Prof. Cristian Teodosiu for all support concerning the microstructural hardening model.

References

[1] Keeler S.P., 1965 Society of Automotive Engineers, Technical paper No. 650535.
[2] Goodwin, G.M., 1968 Society of Automotive Engineers, technical paper no. 680093.
[3] Marciniak, Z. and Kuczynski, K., 1967 Int. J. Mech. Sci. 9, 609-620.
[4] Butuc M.C., A. Barata da Rocha, J.J. Gracio, 2003. J. Mat. Proc. Tech., 142, Issue 3, 714-724.
[5] Banabic D, Comsa DS, Jurco P, Wagner S, Van Houtte P. 2004. Proc. 7th Esaform, 455-458.
[6] Aretz H., 2007. *Int J. Plast*. 23, 798-840.
[7] Cao J, Yao H, Karafillis A and Boyce MC, 2000. *Int J of Plast*. 16, 1105-1129.
[8] Butuc, M.C., Teodosiu, C., Barlat, F., Grácio, J.J., Eur. J. Mech. /A Solids, 2011, 30, 532–546.
[9] Teodosiu C., Hu Z., 1995. Proc. NUMIFORM' 95, pp. 173-182.
[10] Haddadi, H., Bouvier, S.. Banu, M., Maier, C., Teodosiu, C., 2006. Int. J. Plast. 22, 2226-2271.
[11] Barlat, F., Brem, J. C., Yoon, J. W., Chung, K., Dick, R. E., Lege, D. J., Pourboghrat, F., Choi, S. -H. Chu E., 2003 Int. J. Plast. 19, 2003, 1297-1319.
[12] Hiwatashi, S., Bael, A.V., Houtte, P.V., Teodosiu, C., 1998. Int. J. Plasticity, 14, 647-669.
[13] Hoferlin E., Van Bael A., Hiwatashi S.,Van Houtte P, 1998. Proc. 19th Riso Int. Symp. 291-297.
[14] Rauch E. F. and Schmitt J.-H., 1989. Mater. Sci. Eng., A113, 441-448.